Labeling of Monoclonal Antibodies with Samarium-153 for Combined Radioimmunoscintigraphy and Radioimmunotherapy

Graeme R. Boniface, Michael E. Izard, Karen Z. Walker, Diana R. McKay, Peter J. Sorby, J. Harvey Turner, and John G. Morris

Australian Nuclear Science and Technology Organisation, Lucas Heights, NSW, Clinical Immunology Research Centre, University of Sydney, NSW, Fremantle Hospital W.A., Royal Prince Alfred Hospital, Sydney, NSW, Australia

The labeling of a monoclonal antibody K-1-21 with ^{153}Sm has been investigated using the bifunctional chelate cyclic diethylenetriaminepentaacetic acid (DTPA) anhydride. Labeling efficiencies >60% were obtained using high specific activity [^{153}Sm]chloride and a cDTPAa:MAb conjugation ratio of 20:1. The resultant labeled antibody had a s.a. >150 MBq.mg^{-1} and a % retained immunoreactivity >90%. Imaging and biodistribution studies in a rat model demonstrated that specific uptake of ^{153}Sm-K-1-21 into s.c. implants of the target antigen could be clearly detected in scintigrams at 6 days p.i. The specific uptake (1.90 ± 0.45% ID/g, 19.95 ± 2.20 Implant:Blood ratio) compared favorably to ^{131}I- and ^{111}In-labeled K-1-21 (2.52 ± 0.20 and 3.33 ± 0.20% ID/g, 7.69 ± 0.45 and 10.10 ± 0.60 I:B, respectively). Labeling of MAbs with ^{153}Sm for combined scintigraphy/therapy is feasible at clinically appropriate specific activities using cDTPAa, with the resultant conjugates retaining immunoreactivity and in vivo antigen localization.

J Nucl Med 30: 683–691, 1989

Radiolabeled monoclonal antibodies (MAbs) to tumor-associated antigens are widely used for the scintigraphic determination of tumor invasion in a number of clinically important malignancies (*1,2*). The low levels of MAb that are delivered to the tumor following i.v. administration has, however, limited the use of this approach for the systemic therapy of tumors with radiolabeled MAbs (*3*). Despite these limitations, there appears to be some place for radioimmunotherapy with radiolabeled MAbs particularly when confined to intracavitary or lymphatic routes of administration (*4*).

Initial attempts at treating certain tumors with radiolabeled MAbs have used iodine-131 (^{131}I), however, rapid in vivo deiodination of the radiolabel has resulted in low levels of radionuclide being deposited in the target tumor and unwanted radiation to innocent tissues such as the thyroid (*2*). More recently several investigators have used bifunctional chelates for labeling of MAbs with other beta- or alpha-emitting radionuclides, including ^{90}Y (*5,6*), ^{67}Cu (*7*), ^{199}Au (*8*), and ^{212}Bi (*9*), in attempts to produce radioimmunoconjugates with increased in vivo stability and enhanced tumor deposition.

Samarium-153 (^{153}Sm) is a radiolanthanide that possesses excellent physical characteristics for radioimmunotherapy (*10*). It is a beta-emitter [E_{max} = 640 (30%), 710 (50%), and 810 (20%) keV] with a half-life ($t_{½}$) of 1.95 days. In addition it emits a 103 keV gamma ray (28%) that is suitable for gamma camera detection. It can be produced in high yield and high specific activity by neutron activation of enriched ^{152}Sm.

Samarium-153 complexes of citrate, nitrate, and biologically active molecules such as transferrin and bleomycin have been studied as potential tumor-seeking compounds (*11–13*). However, rapid formation of Sm colloids in vivo resulted in high reticuloendothelial (RES) uptake. When complexed to aminocarboxylic acids such as ethylenediaminetetraacetic acid (EDTA)

Received June 7, 1988; revision accepted Jan. 17, 1989.

For reprints contact: G. Boniface, PhD, ANSTO, Private Mail Bag 1, Menai, NSW 2234, Australia.

or diethylenetriaminepentaacetic acid (DTPA), or di- and tetra-phosphonates such as EDTMP or NTMP, stable compounds have been produced (*14–16*). These later complexes of ^{153}Sm have recently been used in animal and human trials for the treatment of skeletal metastases with promising results in reducing tumor pain (*17–19*). A series of other ^{153}Sm complexes have also been synthesized and tested for the combined scintigraphy/therapy of malignant melanoma in nude mice, although results have shown poor tumor localization (*20,21*).

We have investigated the radiolabeling of MAbs with ^{153}Sm using the bifunctional chelate cyclic DTPA anhydride (cDTPAa) and undertaken imaging and biodistribution studies in a rat model system. The antibody chosen for the study was the murine MAb, K-1-21. This antibody reacts with a conformation-dependent epitope present on the constant region of free, but not heavy chain associated kappa light chains (LC) (*22,23*). It also recognizes a tumor-associated antigen (KMA) present on some kappa myeloma and kappa lymphoma cells, and therefore has some clinical potential for treatment of these disorders (*22,24*).

MATERIALS AND METHODS

Monoclonal Antibody Production and Purification

The IgG_1 MAb, K-1-21 (*22*) was purified from ascites by ammonium sulphate fractionation and affinity chromatography on ROW kappa LC conjugated to Sepharose CL-4B beads (Pharmacia, Upsala, Sweden) (see below). Purified antibody was suspended in phosphate buffered saline pH 7.2 (PBS) then concentrated to 20 $mg.ml^{-1}$ for the labeling experiments.

Cyclic DTPA Conjugation to Antibody

All buffers and gels used for radiolabeling and purification were prepared with ion-depleted water Millipore/Waters, Bedford, MA and stored over Chelex-100 (BioRad, Richmond, CA) metal chelating resin. Cyclic DTPA anhydride (Sigma Chemical Co., St. Louis, MO) (cDTPAa) was conjugated to K-1-21 using a modification of the Hnatowich method (*25*). Briefly, cDTPAa was suspended in chloroform (1 $mg.ml^{-1}$). An aliquot containing sufficient cDTPAa for a molar ratio of 10:1-100:1 DTPA:MAb was added to an acid-washed Reactivial (Pierce Chemical Co., Rockford, IL) and evaporated to dryness under a stream of high purity dry nitrogen, K-1-21 MAb (200 μg) was added, the vial was vortexed for 1 min then allowed to stand at room temperature (RT) for 5 min. Several vials were used if more than 1 mg of MAb was conjugated and the solutions mixed as above.

Separation of the DTPA K-1-21 conjugate from free DTPA was achieved by size-exclusion chromatography on a Sephadex G-50 (Pharmacia) (7 × 200 mm) monitored with an in-line uv detector (Pharmacia) at 280 nm.

Preparation of ^{153}Sm

Samarium oxide ($^{152}Sm_2O_3$, 2 mg), isotopically enriched to 98.7% purity, was activated (n, γ) in the Australian Nuclear Science and Technology Organization HIFAR Research Reactor. Irradiation in a neutron flux of 5×10^{13} $n.cm^{-2}.s^{-1}$ for 1 to 5 days yielded ^{153}Sm with specific activities between 12 and 31 $GBq.mg^{-1}$. The activated oxide was dissolved in 6*M* HCl, evaporated to dryness, and redissolved in ultra-pure water. Samarium-153 chloride was either used directly for labeling or passaged through a 2 × 20 mm ion exchange column (AG 1-X8) (BioRad) to produce [^{153}Sm]acetate.

Samarium-153 Labeling of Antibody

Samarium-153 (acetate or chloride) was added to the purified DTPA-conjugated antibody and allowed to stand at RT for 30 min. The labeled antibody was then purified by elution from a P6-DG column (BioRad) (20 × 80 mm). Column elution was monitored with both an in-line solid crystal scintillation detector/counter peaked to the 103 keV gamma emission of ^{153}Sm and 280 nm uv monitor. Total peak radioactivity was determined with an isotope dose calibrator and total protein recovery was quantified by Bradford assay (BioRad). The results were used to accurately quantify the specific activity (s.a.) of the recovered radiolabeled antibody.

HPLC Analysis of Labeled Antibody

Representative samples of purified ^{153}Sm-K-1-21 were analyzed by size exclusion HPLC (Bio-Sil TSK 250 (Bio Rad), 7.5 × 300 mm, 0.2*M* Tris buffer pH 7.0). Column elution (1 $ml.min^{-1}$) was monitored with an in-line 280 nm uv detector and gamma spectrometer. Retention times were compared with protein standards and unlabeled K-1-21 antibody.

Indium-111 Labeling of Antibody

Indium-111 ($^{111}InCl_3$, 185 $MBq.ml^{-1}$) (Mallinckrodt, St. Louis, MO) was converted to the acetate (0.5 *M*, pH 5.5) before conjugation to DTPA-K-1-21 (20:1) and purified as described above.

Iodine-131 Labeling of Antibody

The K-1-21 antibody was iodinated with ^{131}I (8 $GBq.ml^{-1}$ Na ^{131}I) (Amersham, Buckinghamshire, UK) by the iodogen method (*26*). Iodinated antibody was purified from free iodide by passage over a Sephadex G-25 (Pharmacia) column preblocked with 5% BSA.

Preparation of [^{111}In]DTPA and [^{153}Sm]DTPA

Indium-111-DTPA and [^{153}Sm]DTPA were prepared from their respective acetates by reacting 1 mg of DTPA (Na^+ salt) with 37 MBq of radiolabel in 0.15*M* NaCl pH 7. The formation of the respective DTPA complex was confirmed by thin layer chromatography (ITLC-Sg (Gelman Sciences, Ann Arbor, MI) in 85% methanol).

Antigen-Coupled Sepharose Beads

Human kappa (VOR, ROW, or DAL) or lambda (WAT or MOS) LC were purified from the urine of myeloma patients with ammonium sulphate fractionation and gel filtration (ACA-54) (Pharmacia) (*23*). LC were covalently linked to Sepharose 6MB CNBr (Pharmacia) activated beads and used at 15 mg per g of dry beads (for immunoreactivity assay) or 500 μg per ml of swollen gel (animal implant studies) (*27*).

Immunoreactivity Assay

Retained immunoreactivity of radiolabeled antibody conjugates was assessed using a modified in vitro binding assay previously described (*28*). Briefly, 14 × 1.5 ml micro centri-

fuge tubes were blocked with 1% BSA in PBS by incubation at 37°C for 1 hr then washed with PBS. Seven aliquots (100–700 μl) of both kappa (test) and lambda (control) LC coupled Sepharose beads were dispensed into the pre-blocked tubes. Diluted labeled antibody (100 μl, 50-100,000 cpm) was added to each tube and incubated at 37°C for 1.5 hr. The beads were centrifuged at 5,000 *g*, washed with 0.1% BSA (×1), respun and rewashed with PBS (×3) then counted in a gamma counter (127A Riagamma, LKB/Wallac, Sweden) calibrated for the appropriate radionuclide. Samples (100 μl) of the diluted antibody were counted as standards. The specific binding at each gel (antigen) volume was determined by subtracting the control from the test counts and dividing by the standard. The data was graphed as a double inverse plot and analyzed by linear regression to determine the intercept value of the ordinate. This point corresponds to the inverse of % retained immunoreactivity at infinite antigen excess (*29*).

Animal Studies

Male Fisher 334 rats aged 10–15 wk were used for biodistribution and gamma camera studies. Kappa (test) and lambda (control) LC conjugated Sepharose beads (~0.5 ml) were implanted into opposite flanks of each animal under ether anesthesia as previously described (*27*).

Twenty-four hours after the placement of the implants each animal was injected i.p. with radiolabeled K-1-21. L7, a isotypically identical murine MAb of irrelevant specificity was radiolabeled and used as a control in these studies. Three groups of five animals were administered 37 MBq of either ^{153}Sm-K-1-21, ^{111}In-K-1-21 (100 μg MAb, 20:1 cDTPAa:MAb) or ^{131}I-K-1-21 (100 μg). Animals receiving ^{131}I-K-1-21 were fed KI supplemented drinking water from 7 days preinjection to block the thyroid. Further groups of rats were similarly administered [^{153}Sm]acetate, [^{153}Sm]DTPA, [^{111}In]acetate, or [^{111}In]DTPA.

Animals were imaged on a gamma camera (Searle Pho gamma IV) peaked for the appropriate radionuclide at 2 and 6 days postinjection (p.i.). Each animal was placed prone beneath a pinhole collimator, and counts acquired for 5 min. Data was stored by an on-line computer (Digital PDP 11/40) in 64 × 64 matrix.

Following imaging, each animal was exsanguinated, dissected and selective organs counted in a gamma counter peaked for the appropriate radionuclide. Bone marrow radioactivity was distinguished from bone matrix by aspiration of the femoral marrow with saline. Tissue distribution profiles of % injected dose/organ (% ID/organ), % injected dose/g (% ID/g), and tissue/blood ratios (T:B) were generated using a computer biodistribution program. Kappa:lambda implant specificity indices were calculated as previously described (*28*). Data was compared (Student's t-test) for each radiolabel and against the L7 control MAb.

RESULTS

Stability of the Radionuclide

Preliminary experiments produced reasonable labeling of DTPA-conjugated MAb with freshly prepared [^{153}Sm]acetate. When [^{153}Sm]acetate (s.a. 12 GBq.ml^{-1}) was complexed with DTPA-K-1-21 (50:1) at pH 7, a labeling efficiency of 62.7% was achieved (Table 1). A reduction in % labeling efficiency was noted however when [^{153}Sm]acetate was labeled to DTPA-K-1-21 at pH values below and above neutrality.

Labeling efficiency was substantially reduced when the [^{153}Sm]acetate stock solution had been stored for up to a week following production (Table 2). In addition it was found that a substantial amount of the radioactivity was retained on the gel column when the [^{153}Sm]acetate was not fresh. Macroscopic examination of the [^{153}Sm]acetate stock solution revealed that the material had become cloudy and a fine precipitate developed within a week of production. As similar changes in labeling efficiency and precipitate formation were not observed with [^{153}Sm]chloride after a similar storage period (Table 2) it was the radiochemical form chosen for all subsequent labeling experiments.

Effect of Conjugation Ratio and Specific Activity on Labeling Efficiency

As might be expected from theoretical predictions, ^{153}Sm incorporation onto antibody conjugates was found to increase in near linear fashion following either an increase in the s.a. of [^{153}Sm]chloride stock solution or after an increase in the cDTPAa:MAb conjugate ratio (Table 3). Thus a threefold increase in label incorporation occurred when the s.a. of [^{153}Sm]chloride was increased from 12 to 31 GBq.mg^{-1} by irradiation of target material for 5 days instead of 1 day. Use of this material resulted in a conjugate of s.a. between 48.1 and 152.0 MBq.mg^{-1} when cDTPAa:MAb conjugation ratio was increased from 10:1 to 30:1 (Table 3). Using low s.a. [^{153}Sm]chloride stock a conjugate s.a. approaching 100 MBq.mg^{-1} was only achieved above a cDTPAa:MAb conjugation ratio of 50:1.

Using high s.a. [^{153}Sm]chloride and a conjugation ratio of 20:1, routine labeling efficiencies of above 60% were achieved when 200 μg K-1-21 and 40 MBq [^{153}Sm]chloride were used. This translated to a resultant ^{153}Sm-antibody s.a. >150 MBq.mg^{-1}. When scaling up to label amounts of antibody in excess of 1 mg, we found it necessary to employ a multi-vial conjugation procedure due to finding that % labeling efficiency decreased with increased protein added. The multi-vial procedure has resulted in >50% labeling efficiency on numerous occasions and a labeled antibody s.a. routinely above 120 MBq.mg^{-1}.

High performance liquid chromatography (HPLC) analysis of the gel column purified ^{153}Sm-K-1-21 conjugates showed matched 280 nm uv absorbance and radioactive peaks at 4.2 min retention time (Fig. 1). This corresponded to the expected elution time of IgG using protein standards and to that determined for K-1-21 MAb. Only minimal absorbance of radioactivity was demonstrated at the void volume, or at increased retention time when ^{153}Sm-K-1-21 was conjugated at a 20:1 cDTPAa:MAb ratio.

TABLE 1
Effect of pH on the Labeling of K-1-21 with ^{153}Sm

pH	% Labeling efficiency		Specific Activity ^{153}Sm-K-1-21 ($MBq.mg^{-1}$)	
	[^{153}Sm]acetate*	[^{153}Sm]chloride†	[^{153}Sm]acetate*	[^{153}Sm]chloride†
5	12.3	58.0	27.7	109.2
6	28.2	56.0	58.1	107.9
7	62.7	68.5	140.7	133.2
8	34.1	57.8	70.3	118.9
9	27.8	52.1	62.9	101.2

* s.a. of the label 12 $GBq.mg^{-1}$, cDTPAa:MAb conjugation ratio 50:1, 200 μg K-1-21, 40MBq [^{153}Sm]acetate added.
† s.a. of the label 31 $GBq.mg^{-1}$ cDTPAa:MAb conjugation ratio 20:1, 200 μg K-1-21 40MBq [^{153}Sm]chloride added.

Effect of Labeling Conditions on Immunoreactivity

Retained immunoreactivity (i.r.) of ^{153}Sm-labeled K-1-21 conjugates was assessed using an in vitro binding assay to kappa LC immobilized on Sepharose beads. Almost complete retention of i.r. was observed in the ^{153}Sm-K-1-21 conjugates immediately following purification when a conjugation ratio of up to 20:1 cDTPAa:MAb was used (Table 4). Conjugation ratios above this level had a detrimental effect on the i.r. of the antibody such that a conjugation ratio of 50:1 cDTPAa:MAb reduced i.r. to a level of ~50% ($p < 0.05$). When conjugates were prepared at the optimal cDTPAa:MAb ratio of 20:1, i.r. was found to remain unaffected by the amount of ^{153}Sm label attached (up to 150 $MBq.mg^{-1}$) and was similar to that achieved when K-1-21 was labeled with ^{131}I or ^{111}In.

The immunoreactivity of ^{153}Sm-K-1-21 after storage at 4°C was assessed for a period up to 7 days for three different preparations of labeled antibody. In all preparations % retained i.r. diminished with time until ~50% of the full immunoreactivity remained after 7 days storage. This loss of immunoreactivity presumably reflects radiolysis of the ^{153}Sm-labeled antibody.

Animal Biodistribution Studies

The imaging and biodistribution of ^{153}Sm labeled K-1-21 were examined in normal rats bearing s.c. kappa LC (test) and lambda LC (control) antigen-sepharose implants. Two preparations of ^{153}Sm-K-1-21 were produced for biodistribution studies, both were chelated at the optimal cDTPAa:MAb ratio of 20:1, but using different s.a. [^{153}Sm]chloride stock solutions (12 and 31 $GBq.mg^{-1}$). This resulted in preparations of ^{153}Sm-K-1-21 with s.a. of 48 and 120 $MBq.mg^{-1}$. Immunoreactivity remained above 90% following labeling for both preparations. As only minor differences in biodistribution were seen with the two different s.a. preparations of ^{153}Sm-K-1-21, we have reported only the results obtained with ^{153}Sm-K-1-21 of s.a. 48 $MBq.mg^{-1}$. Results were compared with those obtained after injection of ^{131}I-K-1-21 or ^{111}In-K-1-21.

Gamma camera images were taken, without background subtraction, at Day 2 and 6 p.i. (Fig. 2). By Day 2, each type of conjugate showed localization to the kappa rather than the lambda implant. The specific localization became more clearly delineated by Day 6, when blood-pool activity had declined. The images obtained with ^{153}Sm-K-1-21 more closely resembled those obtained with ^{111}In-K-1-21 than with ^{131}I-K-1-21. Both ^{111}In- and ^{153}Sm-labeled antibody showed accumulation within the RES and kidneys, which was not

TABLE 2
Effect of Storage Time of ^{153}Sm Stock on Antibody Labeling Efficiency (Decay Corrected)

Storage period (days)	% Labeling efficiency	
	[^{153}Sm]acetate*	[^{153}Sm]chloride†
0	62.7	68.5
1	26.7	60.2
3	11.0	48.0
6	<5	45.2

* s.a. of the label 12 $GBq.mg^{-1}$, cDTPAa:MAb conjugation ratio 50:1, 200 μg K-1-21, 40 MBq [^{153}Sm]acetate added.
† s.a. of the label 31 $GBq.mg^{-1}$, cDTPAa:MAb conjugation ratio 20:1, 200 μg K-1-21, 40 MBq [^{153}Sm]chloride added.

TABLE 3
Effect of cDTPAa:MAb Conjugation Ratio on the Labeling of MAb with [^{153}Sm]Chloride

Conjugation ratio	Specific activity ^{153}Sm-K-1-21 ($MBq.mg^{-1}$)	
	(a)†	(b)‡
0	<0.1	<0.2
10:1	13.3	48.1
20:1	51.8	114.7
30:1	70.3	152.0
50:1	107.3	—
100:1	118.4	—

* MAb labeled in 0.05 *M* NaCl pH7.
† s.a. of [^{153}Sm]chloride 12 $GBq.mg^{-1}$
‡ s.a. of [^{153}Sm]chloride 31 $GBq.mg^{-1}$

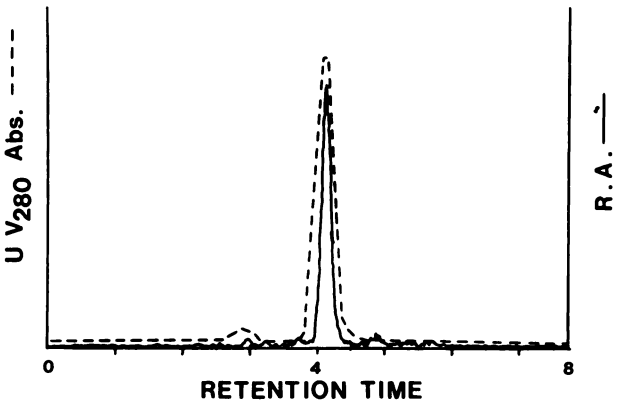

FIGURE 1
Size exclusion HPLC profile of ^{153}Sm-K-1-21 (20:1 cDTPAa:MAb conjugation ratio). Chromatogram on Bio-Sil TSK-250 column, with 0.2*M* Tris buffer pH 7.0 (1 ml.min^{-1}). Radioactivity (R.A.) ——, uv. Absorbance at 280 nm— (arbitrary scale). Void volume at 2.9 min and IgG at 4.2 min retention time.

evident in the ^{131}I antibody images. Skeletal deposition was evident in the ^{153}Sm-K-1-21 scintigrams at Day 6, while the same degree of bone retention was not observed with either ^{131}I or ^{111}In labeled K-1-21.

Biodistribution studies were completed by Day 6 p.i. (Fig. 3). The results confirmed the specific localization of ^{153}Sm-K-1-21 to the kappa implants (1.90 ± 0.18% ID/g) which was significantly higher ($p < 0.01$) than the lambda control (0.80 ± 0.02% ID/g). The kappa:lambda implant specificity index was thus 2.35 ± 0.19, which compares favorably with ^{111}In-K-1-21 (2.44 ± 0.13) but is lower than that determined for ^{131}I-K-1-21 (3.58 ± 0.31). The kappa:lambda specificity index for ^{153}Sm-L7 control was 0.97 ± 0.12.

As suggested by the gamma camera images, the biodistribution of ^{153}Sm-K-1-21 in normal tissues more closely resembled that observed with ^{111}In-K-1-21 than ^{131}I-K-1-21. In particular, ^{153}Sm-K-1-21 accumulated in organs of the RES and in the kidneys in a similar manner to ^{111}In labeled antibody. ^{153}Sm-K-1-21 thus gave nearly equivalent kidney (2.10 ± 0.24 vs. 2.39 ± 0.10), lower splenic (0.65 ± 0.02 vs. 1.41 ± 0.07), but higher hepatic (1.20 ± 0.04 vs. 0.60 ± 0.03) % ID/g estimates than ^{111}In-K-1-21.

Despite similarities in the RES uptake, the biodistribution of ^{153}Sm-K-1-21 also showed significant differences from that of ^{111}In-K-1-21. Firstly, blood clearance of ^{153}Sm-labeled antibody was significantly faster ($p < 0.01$) than that of other conjugates. This resulted in higher Implant:Blood ratios for this radionuclide (19.95 ± 2.20) in comparison to ^{111}In (10.10 ± 0.06) and ^{131}I (7.69 ± 0.45) and clearer delineation of kappa implant uptake from background in the Day 2 scintiphotos. Second, confirming the scintigraphic findings, there was significantly higher ($p < 0.01$) uptake of ^{153}Sm in the bone (femur). The bone uptake was 0.82 ± 0.06% ID/g for ^{153}Sm-K-1-21 in contrast to 0.25 ± 0.02 and 0.09 ± 0.01 % ID/g for ^{111}In and ^{131}I labeled K-1-21, respectively. Counting of the femoral bone marrow aspirates revealed that less than 5% of the ^{153}Sm radioactivity associated with the femur could be recovered by marrow removal, implying that skeletal uptake is osseous rather than marrow associated.

Animals were also injected with [^{153}Sm]acetate or [^{153}Sm]DTPA in order to compare the biodistribution of these complexes with ^{153}Sm-K-1-21 as well as with [^{111}In]acetate or [^{111}In]DTPA. As expected (Fig. 4) both [^{153}Sm]DTPA and [^{111}In]DTPA were rapidly cleared from the body by the kidneys with minimal retention of radioactivity by the implants or other tissues. In contrast the whole-body retention of both [^{153}Sm]acetate and [^{111}In]acetate was much more prolonged. On Day 6 p.i. liver uptake was more pronounced for [^{153}Sm] acetate while splenic and kidney retention was higher with [^{111}In]acetate.

TABLE 4
Retained Immunoreactivity of Radiolabeled K-1-21 Stored at 4°C

Time (days)	Retained Immunoreactivity (%) (Mean ± s.d.)				
	^{131}I-K-1-21* (n = 3)	^{111}In-K-1-21* (n = 3)	^{153}Sm-K-1-21 (a)† (n = 3)	^{153}Sm-K-1-21 (b)‡ (n = 3)	^{153}Sm-K-1-21 (c)§ (n = 2)
0	90.8 ± 2.6	92.5 ± 1.9	92.0 ± 2.8	90.8 ± 2.1	47.7 ± 4.6
1	—	—	86.0 ± 3.1	64.8 ± 3.2	23.5 ± 4.9
2	—	—	68.0 ± 3.6	—	12.8 ± 4.4
7	—	—	45.7 ± 4.1	—	—

* s.a. 370 MBq.mg^{-1}
† s.a. 114 MBq.mg^{-1} ^{153}Sm-K-1-21 labeled with ^{153}Sm-chloride (31 GBq.mg^{-1}) 20:1 cDTPAa:MAb Conjugation ratio.
‡ s.a. 52 MBq.mg^{-1} ^{153}Sm-K-1-21 labeled with ^{153}Sm-chloride (12 GBq.mg^{-1}) 20:1 cDTPAa:MAb Conjugation ratio.
§ s.a. 140 MBq.mg^{-1} ^{153}Sm-K-1-21 labeled with ^{153}Sm-chloride (12 GBq.mg^{-1}) 50:1 cDTPAa:MAb Conjugation ratio.

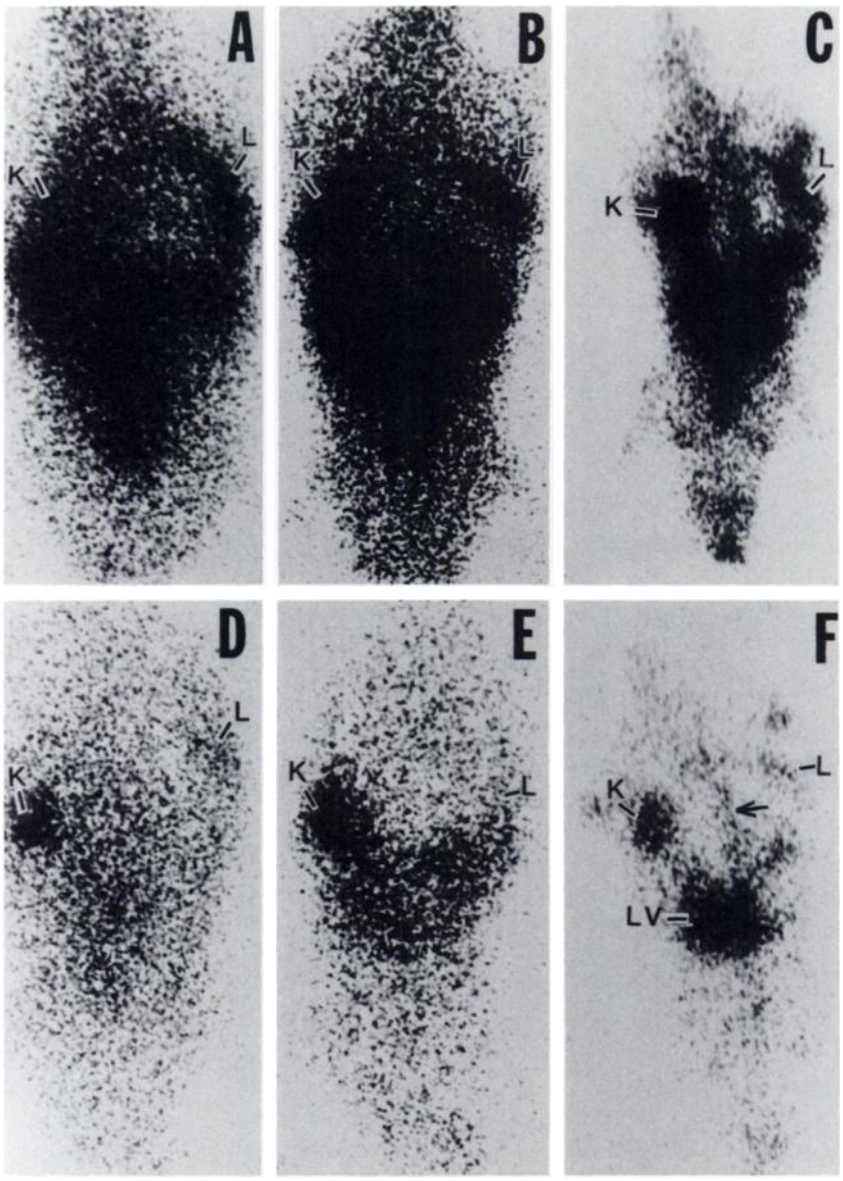

FIGURE 2
Gamma camera scintigrams of Fisher rats injected with ^{131}I-K-1-21, ^{111}In-K-1,21, and ^{153}Sm-K-1-21 at Day 2 (A, B, C, respectively) and 6 (D, E, F, respectively) p.i.. Animals are positioned head down and contain s.c. kappa LC (K) and lambda LC (L) antigen implants. Increased ^{153}Sm-K-1-21 uptake is demonstrated in the liver (LV) and skeleton (arrow) at day 6 p.i. (F) in comparison to ^{131}I-K-1-21 (D) or ^{111}In-K-1-21 (E).

DISCUSSION

Sm(III) is known to form stable complexes with DTPA, although the association constant is somewhat lower than that for the corresponding Ga(III) or In(III) complexes (Log K_M = 22.3, 24.3, and 29.0, respectively) (*30,31*). The association constant reported for Sm(III) is of similar order to that reported for Y(III) (22.0) and therefore radioimmunoconjugates of ^{153}Sm-DTPA-MAb should possess similar in vitro stability to those of the corresponding yttrium-90 DTPA-MAb complex.

These studies have indicated that a stable complex of ^{153}Sm-K-1-21 can indeed be produced at neutral pH using the bifunctional chelate cDTPAa and [^{153}Sm] chloride. Although % labeling efficiency and s.a. were improved by increasing the cDTPAa:MAb conjugation ratio, it was found that an increased loss of i.r. occurred. For optimal retention of i.r., a cDTPAa:MAb conjugation ratio of 20:1 was considered the highest practicable. At this ratio, and using high specific activity [^{153}Sm] chloride (31 GBq.mg^{-1}) ^{153}Sm-K-1-21 of specific activity >150 MBq.mg^{-1} was routinely produced. HPLC analysis of the gel column purified ^{153}Sm-K-1-21 has shown minimal contamination with larger molecular weight species (cross-conjugated antibody or colloid) under these labeling conditions.

Given that the amount of MAb generally administered for optimal clinical tumor imaging is often in the range of 10–50 mg per patient (*32*), these labeling conditions would allow up to 5,000 MBq of ^{153}Sm to be incorporated onto the antibody without significant loss of antibody i.r. from the conjugation procedure. Studies have not yet determined the effect on antibody i.r. from the internal radiation dose from such a thera-

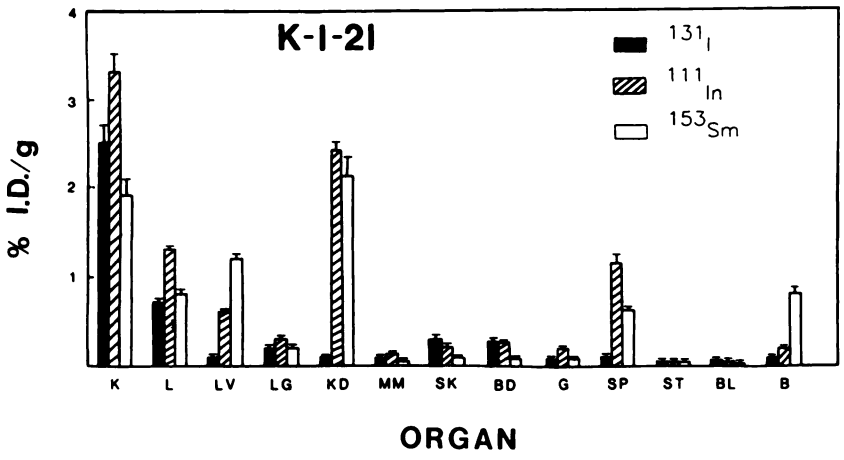

FIGURE 3
Biodistribution profiles (% ID/g) of Fisher rats injected with ^{131}I-, ^{111}In-, and ^{153}Sm labeled K-1-21 6 days p.i. (Mean ± s.e.m., n = 5). Implants: K = kappa LC, L = lambda LC, Organs: LV = liver, LG = lung, KD = kidney, MM = muscle, SK = skin, BD = blood, G = gonads, SP = spleen, ST = stomach, BL = bladder, B = bone.

peutic preparation, although an external gamma dose of 25 kGy has previously been shown to have minimal effect on the i.r. of K-1-21 (unpublished results).

In order to assess the biodistribution of the ^{153}Sm-K-1-21 antibody a rat model as used (*27*). This model employs s.c. implanted antigen-coupled sepharose as an alternative to human tumor xenografts in immunosuppressed or athymic mice. It provides a target with known and constant antigen density, avoiding variations arising from differences in tumor metabolism (*33*). In addition, variations in labeled antibody metabolism and radionuclide deposition by xenografted tumor cells are avoided. These factors are of considerable importance when comparing the localization of antibodies labeled with different radionuclides.

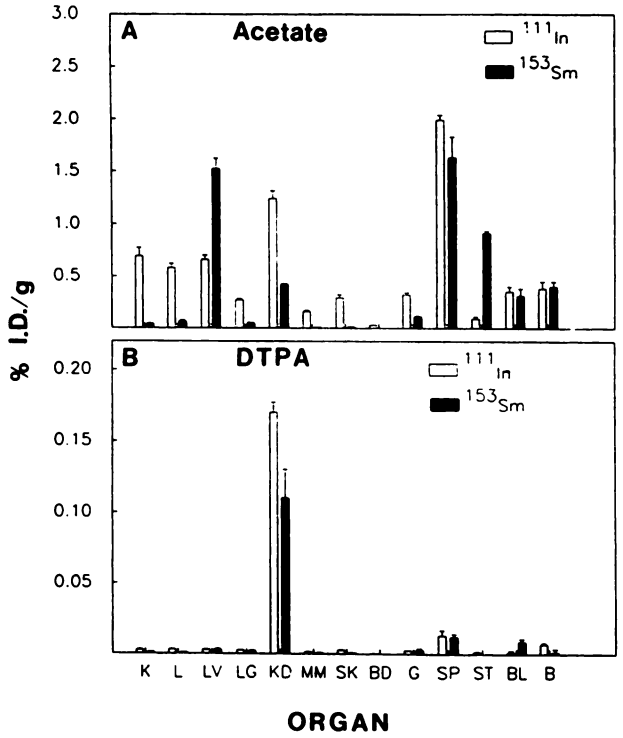

FIGURE 4
Biodistribution profiles (% ID/g) of Fisher rats injected with (A) [^{111}In]acetate or [^{153}Sm]acetate and (B) [^{111}In]DTPA or [^{153}Sm]DTPA 6 days p.i. (Mean ± s.e.m., n = 5). Implants: K = kappa LC, L = lambda LC, Organs: LV = liver, LG = lung, KD = kidney, MM = muscle, SK = skin, BD = blood, G = gonads, SP = spleen, ST = stomach, BL = bladder, B = bone.

This study has clearly shown that ^{153}Sm-K-1-21 will specifically localize to target antigen implants, and that high quality gamma camera images can be obtained of the antibody-implant uptake. The biodistribution pattern is consistent with that of a labeled antibody complex, in contrast to that seen with free [^{153}Sm]acetate or [^{153}Sm]DTPA. The biodistribution profile closely resembles that of ^{111}In-labeled antibody with three notable differences. Firstly, preferential liver uptake and reduced splenic sequestration was evident. Blood clearance was increased, while skeletal retention was more pronounced. These patterns most likely reflect differences in the in vivo stability of the ^{153}Sm-labeled antibody in comparison to that of an identical antibody labeled with ^{111}In.

As noted above, the association constant for Sm-DTPA is lower than for In-DTPA. It is therefore feasible that the resultant ^{153}Sm-DTPA-MAb complex is relatively weaker in vivo than the corresponding ^{111}In-DTPA-MAb complex. The relative in vivo stability is, however, complicated by the role of plasma proteins, which may act to compete for the metal ion attached to MAbs. Whilst it is known that transferrin has a strong affinity for In(III) and this is directly responsible for the loss of 8–9% of the ^{111}In radiolabel per day from labeled antibodies (*5*), the competition by plasma proteins for Sm is less clear. It is known that transferrin does not form a stable complex with Sm ions (*13*), therefore it is unlikely that transferrin will act as a competitive ligand for dissociation of ^{153}Sm from the antibody in vivo. Preliminary experiments have now shown <5% association of ^{153}Sm with transferrin when ^{153}Sm-MAb is incubated in serum for 7 days (Boniface: unpublished data). Serum albumin is known to form complexes with radiolanthanides (*34*) but these are of

relatively low stability. Other recent reports have suggested that, when injected as an ionic complex, ^{153}Sm may form carbonate colloids (*16,20*) with resultant RES sequestration. However, studies with internally labeled MAb have also indicated a predilection of MAb for the liver (*33*). The liver uptake of ^{153}Sm-MAb in our biodistribution studies is therefore most likely a combination of both antibody binding and in vivo dissociation effects.

The uptake of ^{153}Sm in bone is an interesting finding, and one that cannot be explained by the formation of colloid species from in vivo dissociation of ^{153}Sm-MAb. Previous reports have observed the bone sequestration of ^{153}Sm when complexed to ligands of intermediate formation constants, such as EDTA, despite the fact that other metal complexes of these ligands do not normally distribute to bone (*14,16*). It is most likely that there is a direct transchelation of ^{153}Sm from DTPA-antibody to bone matrix and this transchelation becomes more obvious due to the longer blood residence of time ^{153}Sm-MAb than with chelates of ^{153}Sm which are rapidly cleared by the kidneys. Further studies have now commenced to determine in detail the in vivo stability of ^{153}Sm-labeled antibodies, to study the labeling of antibody fragments, and to calculate whole body dosimetry.

In conclusion, it is possible to label monoclonal antibodies with ^{153}Sm and the resultant radioimmunoconjugates retain their immunoreactivity and in vivo antigen localization. Further studies are warranted to determine if ^{153}Sm-labeled antibodies have some clinical value for the radioimmunotherapy of certain tumors.

ACKNOWLEDGMENTS

The authors thank Mr. D. Henderson for help in the production of ^{153}Sm, Ms. S. Stewart for help with the animal studies, and Drs. W. Britton and R. Raison for access to the L7 and K-1-21 antibodies. The aid of technical staff at the Nuclear Medicine Dept, Royal Prince Alfred Hospital with the gamma camera studies is gratefully appreciated. This work was supported in part by a grant from the NSW State Cancer Council.

REFERENCES

1. Carrasquillo JA, Krohn KA, Beamer P, et al. Diagnosis of and therapy for solid tumors with radiolabelled antibodies and immune fragments. *Cancer Treat Rep* 1984; 68:371–378.
2. Larson SM. Radiolabeled monoclonal anti-tumor antibodies in diagnosis and therapy. *J Nucl Med* 1985; 26:538–545.
3. Epenetos AA, Nook D, Durban H, et al. Limitations of radiolabeled monoclonal antibodies for localization of human neoplasms. *Cancer Res* 1986; 46:3183–3191.
4. Courtenay-Luck N, Epenetos AA, Howman KE. Antibody-guided irradiation of malignant lesions; three cases illustrating new method on treatment. *Lancet* 1984; 1441–1443.
5. Hnatowich DJ, Virzi F, Doherty PW. DTPA-coupled antibodies labeled with yttrium-90. *J Nucl Med* 1985; 26:503–509.
6. Washburn LC, Hwa Sun TT, Crook JE, et al. ^{90}Y-labeled monoclonal antibodies for cancer therapy. *Nucl Med Biol* 1986; 13:453–456.
7. Desphande SV, DeNardo SJ, Meares CF, et al. Copper-67-labelled Monoclonal Antibody Lym-1, a potential radiopharmaceutical for cancer therapy: labeling and biodistribution in RAJI tumored mice. *J Nucl Med* 1988; 29:217–225.
8. Anderson P, Vaughan ATM, Varley NR. Antibodies labeled with ^{199}Au: potential of ^{199}Au for Radioimmunotherapy. *Nucl Med Biol* 1988; 15:293–297.
9. Scheinberg DA, Strand M. Leukemic cell targeting and therapy by monoclonal antibody in a mouse model system. *Cancer Res* 1982; 42:44–49.
10. Ehrhardt GJ, Ketring AR, Volkert WA. Production of Sm-153 for radiotherapeutic applications. *J Labelled Comp* 1986; 23:1370.
11. Hisada K, Ando A. Radiolanthanides as promising tumour scanning agents. *J Nucl Med* 1973; 14:615–617.
12. Woolfenden JM, Hall JN, Barker HB, et al. [^{153}Sm] citrate for tumour and abscess localization. *Int J Nucl Med Biol* 1983; 10:251–256.
13. Tse JW, Noujaim AA, Wiebe LI. [^{153}Sm]Samarium complexes as radiopharmaceuticals [Abstract]. *Fourth Int Symp on Radiopharm Chem* 1982; 278.
14. Karika K, Pal I, Tarjan G, et al. Radioactive samarium complexes (^{153}Sm-EDTA and ^{153}Sm-DTPA) in medical scintigraphy. *Proc IAEA Symp: Medical radioisotope scintigraphy.* IAEA-SM-164/51; Monte Carlo, 1972: 457–465.
15. Goeckeler WF, Troutner DE, Volkert WA, et al. ^{153}Sm radiotherapeutic bone agents. *Nucl Med Biol* 1986; 13:479–482.
16. O'Mara RE, McAfee JG, Subramanian G. Rare earth nuclides as potential agents for skeletal imaging. *J Nucl Med* 1969; 10:49–51.
17. Corwin LA, Lattimer JC, Goeckeler WF, et al. Sm-153 EDTMP treatment of spontaneous canine bone tumors. *J Nucl Med* 1986; 27:986–987.
18. Goeckeler WF, Edwards B, Volkert WA, et al. Skeletal localization of samarium-153 chelates: potential therapeutic bone agents. *J Nucl Med* 1987; 28:495–504.
19. Turner JH, Hoffman RF, Martindale AA, et al. Samarium-153 EDTMP therapy dosimetry and SPECT in cancer patients with disseminated skeletal metastasis [Abstract]. *J Nucl Med* 1988; 29:762.
20. Turner JH, Martindale AA, De Witt GC, et al. Samarium-153 chelate localization in malignant melanoma. *Eur J Nucl Med* 1987; 13:432–438.
21. Turner JH, Martindale AA, De Witt GC, et al. Tumour localisation of Samarium-153 chelates in malignant melanoma. *J Labelled Comp and Radiopharm* 1986; 13:1367–1369.
22. Boux HA, Raison RL, Walker KZ, et al. A tumour-associated antigen specific for human kappa myeloma cells. *J Exp Med* 1983; 158:1769–1774.
23. Raison RL, Boux HA. Conformational dependence of a monoclonal antibody defined epitope on human kappa chains. *Mol Immunol* 1985; 22:1393–1398.

24. Goodnow CC, Raison RL. Structural analysis of the myeloma-associated membrane KMA. *J Immunol* 1985; 135:1276–1280.
25. Hnatowich DJ, Childs RL, Lanteigne D, et al. The preparation of DTPA-coupled antibodies radiolabeled with metallic radionuclides: an improved method. *J Immunol Meth* 1983; 65:147–157.
26. Miller WT, Smith JFG. Protein iodination using iodogen. *Int J Appl Radiat Isot* 1983; 34:639–641.
27. Walker KZ, Seymour-Munn K, Towson J, et al. Radioimmunodetection and selective delivery of radiation in a rat model system: comparison of intact and fragmented antibody. *Nucl Med Res Comm* 1988: 9:517–526.
28. Walker KZ, Seymour-Munn K, Keech FK, et al. A rat model system for radioimmunodetection of kappa myeloma antigen on malignant B cells. *Eur J Nucl Med* 1987; 12:461–467
29. Lindmo T, Boven E, Cuttitta F, et al. Determination of the immunoreactive fraction of radiolabelled monoclonal antibodies by linear extrapolation to binding at infinite antigen excess. *J Immunol Meth* 1984; 72:77–89.
30. Moeller T, Thomson LC. Observations on the rare earths LXXV. The stabilities of diethylenetriaminepentaacetic acid chelates. *J Inorgan Nucl Chem* 1962; 24:499–510.
31. Taliaferro CH, Motekaitis RJ, Martel AE. New multidentate ligands 22. N,N′-Dipyridoxyleneethylenediamine-N,N′-diacetic acid: a new chelating ligand for trivalent metal ions. *Inorgan Chem* 1984; 23:1188–1192.
32. Carrasquillo JA, Abrams PG, Schroff RW, et al. Effect of antibody dose on the imaging and biodistribution of indium-111 9.2.27 antimelanoma monoclonal antibody. *J Nucl Med* 1988; 29:39–47.
33. Sands H, Jones PL. Methods for the study of the metabolism of radiolabelled monoclonal antibodies by liver and tumor. *J Nucl Med* 1987; 28:390–398.
34. Schomaker K, Mocker D, Munze R, Beyer G-J. Stabilities of lanthanide-protein complexes. *Appl Radiat Isot* 1988; 39:261–264.